

ANESTHESIOLOGY

Dynamic Cortical Connectivity during General Anesthesia in Surgical Patients

Phillip E. Vlisides, M.D., Duan Li, Ph.D.,
Mackenzie Zierau, Andrew P. Lapointe, M.Sc.,
Ka I. Ip, M.S., Amy M. McKinney, M.A.,
George A. Mashour, M.D., Ph.D.

ANESTHESIOLOGY 2019; 130:885–97

The brain is the primary target for the anesthetic endpoints of unconsciousness and amnesia. However, unlike other major organ systems, there is no standard monitor for the brain in the perioperative period. This striking gap in clinical care is due to our incomplete understanding of the neural correlates of consciousness. One principled approach to addressing such knowledge gaps is to link drug-specific electroencephalographic signatures with neural circuit-level mechanisms of arousal states.^{1,2} A complementary approach is to search for state-specific signatures that reflect neural correlates of conscious experience. The latter may help establish agent-invariant signatures that can be used for routine perioperative brain monitoring. One such candidate signature, corticocortical connectivity, has been presented as a key discriminator between consciousness and anesthesia in humans.^{3,4} Indeed, data suggest that measures of frontal-parietal connectivity can reflect anesthetic-induced unconsciousness due to a diverse array of agents.^{3,5,6}

Despite these encouraging findings, important questions remain unanswered. First, it is unclear if functional connectivity measures can be pragmatically obtained for “real-world” monitoring in the perioperative period. Second, it is unknown if such connectivity measures successfully differentiate between arousal states in a clinical setting. Third, cortical oscillations have been found in animal studies to shift dynamically during anesthesia.^{7,8} However, clinical evidence is required to support (or refute) preliminary basic

ABSTRACT

Background: Functional connectivity across the cortex has been posited to be important for consciousness and anesthesia, but functional connectivity patterns during the course of surgery and general anesthesia are unknown. The authors tested the hypothesis that disrupted cortical connectivity patterns would correlate with surgical anesthesia.

Methods: Surgical patients (n = 53) were recruited for study participation. Whole-scalp (16-channel) wireless electroencephalographic data were prospectively collected throughout the perioperative period. Functional connectivity was assessed using weighted phase lag index. During anesthetic maintenance, the temporal dynamics of connectivity states were characterized via Markov chain analysis, and state transition probabilities were quantified.

Results: Compared to baseline (weighted phase lag index, 0.163, ± 0.091), alpha frontal-parietal connectivity was not significantly different across the remaining anesthetic and perioperative epochs, ranging from 0.100 (± 0.041) to 0.218 (± 0.136) ($P > 0.05$ for all time periods). In contrast, there were significant increases in alpha prefrontal-frontal connectivity (peak = 0.201 [0.154, 0.248]; $P < 0.001$), theta prefrontal-frontal connectivity (peak = 0.137 [0.091, 0.182]; $P < 0.001$), and theta frontal-parietal connectivity (peak = 0.128 [0.084, 0.173]; $P < 0.001$) during anesthetic maintenance. Additionally, shifts occurred between states of high prefrontal-frontal connectivity (alpha, beta) with suppressed frontal-parietal connectivity, and high frontal-parietal connectivity (alpha, theta) with reduced prefrontal-frontal connectivity. These shifts occurred in a nonrandom manner ($P < 0.05$ compared to random transitions), suggesting structured transitions of connectivity during general anesthesia.

Conclusions: Functional connectivity patterns dynamically shift during surgery and general anesthesia but do so in a structured way. Thus, a single measure of functional connectivity will likely not be a reliable correlate of surgical anesthesia.

(*ANESTHESIOLOGY* 2019; 130:885–97)

EDITOR'S PERSPECTIVE

What We Already Know about This Topic

- Animal data, along with recent human observations (in this issue of *ANESTHESIOLOGY**), suggest that cortical oscillations and connectivity shift dynamically during what appears to be stable general anesthesia
- Clinical evidence in the perioperative setting to support these observations is currently lacking

What This Article Tells Us That Is New

- During anesthesia and surgery, cortical networks display a dynamic interplay among brain states, rather than a static equilibrium
- These findings suggest that a single measure of connectivity may not be a reliable correlate of surgical anesthesia depth

This article is accompanied by an editorial on p. 861. *See article on page 870. Supplemental Digital Content is available for this article. Direct URL citations appear in the printed text and are available in both the HTML and PDF versions of this article. Links to the digital files are provided in the HTML text of this article on the Journal's Web site (www.anesthesiology.org). P.E.V. and D.L. contributed equally to this manuscript.

Submitted for publication July 9, 2018. Accepted for publication February 1, 2019. From the Department of Anesthesiology (P.E.V., D.L., M.Z., A.P.L., K.I.I., A.M.M., G.A.M.), the Center for Consciousness Science (P.E.V., D.L., G.A.M.) and the Neuroscience Graduate Program (G.A.M.), University of Michigan Medical School Ann Arbor, Michigan; and the Department of Psychology, University of Michigan, Ann Arbor, Michigan (K.I.I.).

Copyright © 2019, the American Society of Anesthesiologists, Inc. Wolters Kluwer Health, Inc. All Rights Reserved. *Anesthesiology* 2019; 130:885–97

science findings.⁷ To resolve these questions for neuroscience and anesthesiology, further clinical investigation is required.

The objective of this study was to assess the clinical relevance of brain connectivity patterns in the perioperative setting. Our primary hypothesis was that functional connectivity between frontal and parietal cortices would be depressed during general anesthesia and would increase upon recovery. A secondary aim was to assess for dynamic shifts in cortical connectivity during anesthetic maintenance. In this context, anesthetic maintenance was defined as epochs with minimum alveolar concentration (MAC) greater than or equal to 0.7. Behavioral responsiveness was not assessed during anesthetic maintenance in this study.

Materials and Methods

This was a prospective observational study assessing neurophysiologic patterns in surgical patients. The study was approved by the University of Michigan Medical School Institutional Review Board (Ann Arbor, Michigan; HUM00113764), and written informed consent was obtained from all participants prior to enrollment. All study procedures were conducted at Michigan Medicine (Ann Arbor, Michigan), and participants were enrolled from March 2017 to August 2017.

Study Population

Adult patients (18 yr or older) presenting for surgery requiring general anesthesia were approached for study participation. Exclusion criteria included the following: emergency surgery, surgery involving the head and neck, known difficult airway, non-English speaking, or enrolled in a conflicting research study.

Anesthetic and Perioperative Management

The goal of this study was to assess connectivity patterns in a real-world surgical setting, independently of any specific anesthetic regimen. Thus, anesthetic and perioperative management proceeded as clinically indicated; no research protocol was implemented other than electroencephalographic data acquisition as described in the following sections. All patients underwent induction of general anesthesia with propofol, and general anesthesia was maintained based on the chosen drug regimen of anesthesia teams, often with multiple agents (as described below).

Electroencephalographic Data Acquisition

The electroencephalogram was recorded from 16 silver/silver chloride scalp electrodes using the Mobile-72 wireless system (Cognionics Inc., USA; see Supplemental Digital Content 1, <http://links.lww.com/ALN/B912>, for the corresponding 10 to 20 system montage). Head circumference was measured to assure the proper sized cap was utilized.

Measurements from nasion (bridge of the nose) toinion (occipital protuberance) were then taken along with measurements between the preauricular notches. Finally, 50% of the total length from the two aforementioned measurements was used to properly align Cz. Data recorded were referenced to the mastoid and sampled at 500 samples per second. Impedances were maintained less than 100 k Ω during recording per manufacturer recommendations. Upon entry into the operating room, impedance levels were reassessed and corrected accordingly during surgery and throughout the perioperative period. The electroencephalographic recording computer was synchronized with the electronic medical record in order to timestamp critical events. Critical events depicted in manuscript figures (e.g., induction, loss of consciousness, extubation) were manually recorded by study team members who remained in the operating room.

Electroencephalography Analysis

The raw electroencephalographic signals were exported into MATLAB (version 2017a; MathWorks, Inc., USA), and down-sampled to 250 Hz. We then performed two lines of analysis. First, in terms of the primary outcome, we investigated cortical oscillatory and connectivity changes across clinically relevant perioperative periods with different levels of consciousness (described in Epoch Selection and Preprocessing section). Second, in terms of a secondary and exploratory outcome, we focused solely on the anesthetic maintenance phase to investigate whether cortical connectivity patterns displayed static or dynamic properties during this period.

Epoch Selection and Preprocessing

Nine clinically relevant epochs were selected as displayed in figure 1, and the strategies for spectral and connectivity data abstraction for each epoch are included in table 1. The criteria for epoch selection included the following: (1) using data as close as possible to each clinically relevant event; and (2) having at least one usable channel in each area of interest (prefrontal: Fp1, Fp2; frontal: F5, F6, Fz; parietal: P5, P6, Pz).

During preoxygenation, participants were instructed to keep their eyes closed. After induction, loss of consciousness was assessed clinically by asking participants to squeeze the hand of a research team member prior to neuromuscular blockade. For periextubation data, time points were chosen that would allow for clean data abstraction (particularly in the setting of movement) while remaining reasonably close to the extubation event. Based on data review, time windows within 3 min and 6 min were chosen for pre- and postextubation, respectively. Postanesthesia care unit data were obtained from a 2-min eyes-closed period; consistently artifact-free data available for abstraction were taken from 30- to 60-s epochs as outlined in table 1. These data were obtained after the patient was deemed stable for assessment per clinical staff, which

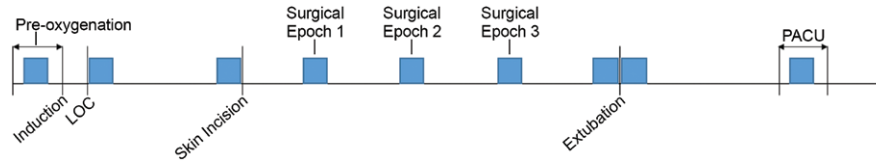


Fig. 1. Study epochs across the perioperative period. *Blue squares* represent the time periods from which electroencephalographic data were abstracted. LOC, loss of consciousness; PACU, postanesthesia care unit; Surgical Epoch 1, data from 25% surgical completion; Surgical Epoch 2, data from 50% surgical completion; Surgical Epoch 3, data from 75% surgical completion.

Table 1. Data Epoch Selection and Characteristics

Epochs	Data Abstraction Characteristics	Sample Size
Preoxygenation	30–60 s from preoxygenation period	n = 44
LOC	1-min segment within 2 min after LOC	n = 46
Preincision	1-min segment prior to skin incision	n = 46
Surgery 1st quarter	1-min segment at 25% surgical completion	n = 49
Surgery 2nd quarter	1-min segment at 50% surgical completion	n = 50
Surgery 3rd quarter	1-min segment at 75% surgical completion	n = 50
Preextubation	1-min segment within 3 min of extubation	n = 39
Postextubation	1-min segment within 6 min after extubation	n = 38
PACU	30–60 s eyes-closed period after PACU arrival	n = 45

Sample size indicates the number of participants whose data were available for each data epoch.

LOC, loss of consciousness; PACU, postanesthesia care unit.

occurred, on average, 24.7 (± 11.6) min after postanesthesia care unit admission.

For each epoch, the electroencephalographic signals were preprocessed in a stepwise manner. First, bad channels with obvious artifacts were removed by visual inspection. Second, the signals were detrended using a local linear regression method with a 10-s window at a 5-s step size in Chronux analysis toolbox⁹ and lowpass filtered at 55 Hz via a fifth-order Butterworth filter using a zero-phase forward and reverse algorithm. Third, the signals were further examined by visual inspection of the waveform and spectrogram, and independent component analysis was applied to remove the components representing cardiac artifact, eye movement, muscle movement, and other artifacts if present, using extended-Infomax algorithm in EEGLAB toolbox.¹⁰ For dynamic connectivity analysis (described further below) the first two preprocessing steps were carried out in the same manner, then noisy data segments were detected and rejected as follows: the signals were divided into 2-s windows, and the 2-s data window was rejected if: (1) its average amplitude was more than four times the average amplitude, or its SD was greater than two times the SD value of the whole signal; and (2) the aforementioned was present in at least one channel. This step rejected $14.6 \pm 13.6\%$ (minimum–maximum, 0 to 56.4%) of the data across the participants, mainly due to electrocautery artifacts.

Spectral Analysis

The power spectrograms were estimated using the multitaper method in Chronux analysis toolbox⁹ with window length equal to 2 s with 50% overlap, time-bandwidth product equal to 2, number of tapers equal to 3. We focused on the cortical power in prefrontal (averaged across Fp1, Fp2), frontal (averaged across F5, F6, Fz), and parietal (averaged across P5, P6, Pz) regions. The group-level spectrogram was obtained by (median) averaging the spectrograms from all available participants and concatenating the nine epochs previously described.

Estimation of Functional Connectivity

The functional connectivity was estimated using weighted phase lag index,¹¹ which is a measure of phase synchronization less affected by volume conduction and reference montage by accounting for only nonzero phase lead/lag relationships.^{11,12} The weighted phase lag index is a measure of how well the instantaneous phases of two signals are phase-locked to each other. If the instantaneous phase of one signal consistently leads or lags those of another signal, the phases are considered locked, and weighted phase lag index is equal to 1; on the other hand, if the phase lead/lag relationship of two signals is random, the weighted phase lag index value will be low. If there is no phase difference

between the two signals, the weighted phase lag index value will be 0.

For implementation, the electroencephalographic signals were divided into 30-s windows at a 10-s step size, which was further divided into 2-s subwindows with 50% overlapping. For each subwindow, the cross-spectral density was estimated using the multitaper method,⁹ with time-bandwidth product equal to 2 and the number of tapers equal to 3; from these repetitions the weighted phase lag index values were estimated as a function of frequency, using a custom-written function adapted from the Fieldtrip toolbox.¹³ To mitigate the potential bias of the weighted phase lag index measure, surrogate data were generated by the trial-shuffling method, from which the weighted phase lag index was calculated and subtracted from the original weighted phase lag index as the final estimation of functional connectivity.¹⁴

In this study, we focused on the cortical connectivity among a few regions of interest, *i.e.*, frontal-parietal connectivity as the averaged weighted phase lag index across the combinations between F5, F6, Fz and P5, P6, Pz, and prefrontal-frontal connectivity as the averaged weighted phase lag index across the combinations between Fp1, Fp2 and F5, F6, Fz. Connectivity across prefrontal-frontal channels was analyzed because this region is implicated in anesthetic-induced unconsciousness (*via* highly synchronized thalamocortical oscillations).^{15,16} For statistical comparisons, the mean frontal-parietal and prefrontal-frontal connectivity were calculated in bandwidths with apparent changes throughout different perioperative epochs (delta [0.5 to 3 Hz], theta [3 to 7 Hz], and alpha [7 to 15 Hz]; see Results section), which were then averaged across all of the time windows in each studied epoch for each participant.

Dynamic Connectivity Analysis during Surgical Anesthesia

To assess for evidence of dynamic cortical connectivity during surgical anesthesia, the temporal variations of cortical connectivity were analyzed during the anesthetic maintenance phase. For the purpose of this analysis, the anesthetic maintenance phase was defined as 30 s after skin incision to the last MAC of 0.7 toward the end of surgery. The value of 0.7 was chosen as a clinically relevant lower-limit of surgical anesthesia for preventing intraoperative awareness with explicit recall.¹⁷ MAC levels are age-adjusted and account for multiple, simultaneous anesthetic agents per previously published algorithms.¹⁸ The event mark for skin incision was not available for three participants; in these cases, 2 min after intubation ($n = 2$) and loss of consciousness ($n = 1$) were used as surrogate markers based on data availability. After carrying out the preprocessing steps described above (see Epoch Selection and Preprocessing), analysis was performed on $n = 45$ participants; 8 of 53 participants (15.1%) were excluded due to bad or incomplete

electroencephalographic recordings ($n = 5$) or insufficient MAC data ($n = 3$). The frequency-resolved frontal-parietal and prefrontal-frontal connectivity were estimated with a window size of 30 s at a 10-s step size for each participant. As the presence of burst suppression precludes reliable estimation of functional cortical connectivity, time windows with suppression ratio greater than 20% were excluded. Segmentation and quantification of burst and suppression were performed using previously described methods.¹⁹ Briefly, the burst and suppression episodes were detected based on instantaneous power at 5 to 30 Hz followed by applying a threshold determined from manually labeled suppression periods, thus yielding a binary series of burst and suppression states, from which the suppression ratio was calculated as percentage of suppression time in each 30-s binary series with a 20-s overlap. Only the electroencephalographic time windows with suppression ratio less than 20% were included for the subsequent connectivity analysis.

The connectivity pattern so obtained was a 140-dimensional vector (each has 70 frequency estimates for 0.5 to 35 Hz), which was aggregated across all participants and subjected to principal component analysis for dimensionality reduction. By principal component analysis, we reduced the original 140-dimensional to M -dimensional feature, while maximally preserving the amount of variation from the original connectivity pattern. The M -dimensional connectivity patterns were then classified into N_c clusters using k-means algorithm with squared Euclidean distance and 100 replications of the initial centroids. The number of clusters (N_c), and the number of retained principal components (M) was determined by the stability index that estimates the normalized minimum Hamming distance between different clustering solutions for the studied dataset,^{20,21} the amount of explained variance by the retained principal components, and the interpretability of the clustering results (see Supplemental Digital Content 2, <http://links.lww.com/ALN/B913>). Each cluster can be regarded as a connectivity state characterized by distinct spectral and spatial properties. Besides these N_c connectivity states, we defined an additional state as “BS” that contains all the windows with burst suppression. Thus, we obtained the connectivity state time series for consecutive time windows for each participant.

Finally, to evaluate the temporal dynamics of the connectivity state time series, we quantified the occurrence rate of a given state together with the distribution of dwell time for each state. The former is defined as the fraction of time spent in each connectivity state, while the latter measures the temporal durations of each state visit. Furthermore, to investigate how cortical connectivity transitions among different states, we assumed the connectivity state time series to be a Markov chain (*i.e.*, the state transition depends only on the current state).^{7,21} We counted the number of times each participant stayed in a certain brain connectivity state (defined as the cortical connectivity at time $t+1$ remaining within the

same state as time t) as well as the number of transitions to other states. Based on prior studies,^{7,21} we hypothesized that cortical connectivity would be persistent—or “sticky”—and reside in the same state. Furthermore, we hypothesized that state transitions would be much less frequent and uneven across states and participants. The analysis was performed in two ways. First, at a participant level, all states were aggregated and cumulative times spent in the same state i ($i = 1, 2, \dots, N_c + 1$) were calculated. The number of transitions to any of the other states, j ($j = 1, 2, \dots, N_c + 1$, but $j \neq i$) was also calculated. Next, probabilities of state stays and transitions were each calculated by dividing the total times of state stays and transitions for each participant. Second, following previous studies,^{21–25} the transition probability for each pair of connectivity states was calculated using all participants. The transition probability is the likelihood that the current state will transition to another state at a future time at the group level. For the transition from State i to State j ($i, j = 1, 2, \dots, N_c + 1$), the transition probability was estimated by counting the number of this transition divided by the total number of all state transitions (including state persistencies) across all participants, and the matrix so obtained represented the transition probability for each pair of connectivity state, with all elements of the matrix summing up to 1.

Statistical Analysis

No *a priori* statistical power calculation was conducted to guide sample size. The sample size of 53 patients (maximum of 50 for any given data epoch, table 1) is consistent with (and exceeds) previous efforts investigating whole-scalp oscillatory electroencephalographic patterns in adult surgical patients.^{5,26,27}

For static connectivity analysis, statistical comparisons were performed using linear mixed models (IBM SPSS Statistics version 24.0 for Windows; IBM Corp. USA) to test (1) the difference between the nine studied epochs for both frontal–parietal and prefrontal–frontal connectivity measures, and (2) the difference between frontal–parietal and prefrontal–frontal connectivity. Linear mixed modeling analysis offers more flexibility with missing values and accounts for individual differences by including a random intercept associated with each participant. For the connectivity values at each frequency band, the fixed effects included the studied epoch, region pair, and the interaction between them. We used restricted maximum likelihood estimation and variance components as covariance structure of random effects. The *post hoc* pairwise comparisons were performed between each studied epoch relative to the baseline preoxygenation epoch and between frontal–parietal and prefrontal–frontal connectivity if the regional pair fixed effects were statistically significant ($P < 0.05$). The mean and 95% CI values of the estimated difference along with the two-sided, Bonferroni-corrected P values were reported in the Results section.

For dynamic connectivity analysis, the statistical analyses were performed using MATLAB. The normality of data distribution was evaluated by Lilliefors corrected Kolmogorov–Smirnov test. To compare the likelihood of remaining in the same state or switching to a different state, paired-sample two-sided t test was used to compare the probabilities of state stays and state switches across the participants. Before the test, the null hypothesis of normality of distribution was not rejected at the 5% significance level. To test the statistical significance of state transitions between each pair of connectivity states, a multistep surrogate data analysis was performed. First, $N = 1,000$ surrogate time series were generated by randomly shuffling the connectivity state time series for each participant, which permuted the temporal order of the state occurrence while keeping the occurrence rate of the states. Second, regarding between-state transitions, we generated $N = 1,000$ surrogate time series by randomly permutating the retained state time series (including only state switches) after removing the state stays, with the constraint of each state’s occurrence rate across all participants. With each surrogate time series, the transition probability was then calculated for each pair of connectivity states, and a state transition was deemed statistically significant by comparing the original transition probability with those from surrogate data. The significance value was obtained through the cumulative distribution

function, $p = 1 - \int_{-\infty}^{\alpha} p_{\text{surro}}(h) dh$, where α denotes the original transition probability and $p_{\text{surro}}(h)$ denotes the estimated normal distribution if the null hypothesis of normality of surrogate data could not be rejected, or empirical surrogate distribution otherwise.²⁸ Across all the studied state transitions, the false discovery rate-adjusted $P < 0.05$ was considered significant.

Results

In total, 97 patients were screened for eligibility and enrollment. Of the 65 enrolled patients, 12 (18.5%) were withdrawn, leaving 53 participants who completed the study and were included for analysis. Demographic and surgical characteristics are presented in table 2. Mean participant age was 50 ± 17 , and cases spanned various subspecialties. Anesthetic maintenance regimens and MAC values are presented in Supplemental Digital Content 3, <http://links.lww.com/ALN/B914>. In total, 98% of all MAC values were at least 0.7 or greater during the evaluated anesthetic maintenance phase (see Supplemental Digital Content 3, fig. 1A, <http://links.lww.com/ALN/B914>). Individual anesthetics varied both among patients and during individual cases during anesthetic maintenance, though the majority of patients received nitrous oxide paired with either sevoflurane or isoflurane (see Supplemental Digital Content 3, fig. 1B, <http://links.lww.com/ALN/B914>).

Table 2. Participant Characteristics

Surgical Patients (N = 53)	
Age, yr, (mean \pm SD)	50 \pm 17
Male sex, No. (%)	29 (54.7)
Race, No. (%)	
White	46 (86.8)
Black	4 (7.5)
Other	3 (5.7)
Ethnicity, No. (%)	
Non-Hispanic	46 (86.8)
Other/unknown	4 (7.5)
Hispanic	3 (5.7)
Type of surgery, n (%)	
Urology	26 (49.1)
Orthopedic	10 (18.9)
Surgical oncology	6 (11.3)
Plastics	6 (11.3)
Neurosurgery	3 (5.7)
Minimally invasive surgery	2 (3.8)

Spectral Analysis

Group-level spectrograms are presented in figure 2. Most notably, spectral analysis revealed increases in alpha and theta power during surgery, with alpha increases noted most prominently in the prefrontal and frontal channels (fig. 2). Gamma power was increased both before and after extubation, which was decreased in the postanesthesia care unit in all channels compared to postextubation levels (fig. 2).

Cortical Connectivity across the Perioperative Period

Group-level connectivity data from the perioperative period are presented in figure 3. The cortical connectivity during preoxygenation was characterized by a predominance of frontal–parietal connectivity in the alpha band. However, compared to preoxygenation baseline (weighted phase lag index, 0.163 ± 0.091), alpha frontal–parietal connectivity was not significantly different across all remaining epochs (range, 0.100 ± 0.041 to 0.218 ± 0.135 ; $P > 0.05$ for all comparisons). With induction, delta connectivity was increased compared to baseline for both frontal–parietal (0.083 [$0.042, 0.124$]; $P < 0.001$) and prefrontal–frontal channels (0.154 [$0.113, 0.195$]; $P < 0.001$; prefrontal–frontal *vs.* frontal–parietal: 0.066 [$0.026, 0.107$]; $P = 0.011$). Prefrontal–frontal alpha connectivity increased during anesthetic and surgical epochs (preincision: 0.201 [$0.154, 0.248$]; $P < 0.001$; first surgical epoch: 0.169 [$0.123, 0.215$]; $P < 0.001$; second surgical epoch: 0.178 [$0.132, 0.224$]; $P < 0.001$; third surgical epoch: 0.173 [$0.127, 0.219$]; $P < 0.001$). Compared to frontal–parietal channels, prefrontal–frontal alpha connectivity was also stronger throughout the anesthetic and surgical periods (preincision: 0.135 [$0.089, 0.181$]; $P < 0.001$; first surgical epoch: 0.077 [$0.032, 0.122$]; $P = 0.007$; second surgical epoch: 0.067 [$0.022, 0.111$]; $P = 0.030$; third surgical epoch: 0.078 [$0.033, 0.122$]; $P = 0.006$). Additionally,

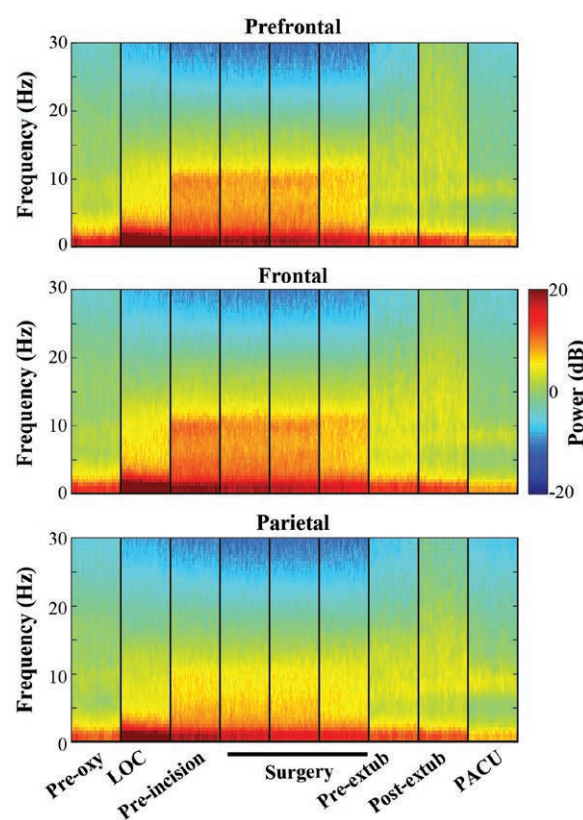


Fig. 2. Group-level power spectrogram, generated by concatenating the nine clinically relevant epochs and averaging median power values (decibels, dB) across all available patients. For each patient, the power spectrogram was averaged over prefrontal (Fp1, Fp2), frontal (F5, F6, Fz), and parietal (P5, P6, Pz) channels. LOC, loss of consciousness; PACU, postanesthesia care unit; pre-oxy, preoxygenation; pre-extub, preextubation; post-extub, postextubation.

there was an increase in theta connectivity during anesthetic and surgical epochs in both frontal–parietal (preincision: 0.114 [$0.068, 0.160$]; $P < 0.001$; first surgical epoch: 0.112 [$0.067, 0.157$]; $P < 0.001$; second surgical epoch: 0.128 [$0.084, 0.173$]; $P < 0.001$; third surgical epoch: 0.088 [$0.043, 0.133$]; $P = 0.001$) and prefrontal–frontal channels (preincision: 0.117 [$0.071, 0.162$]; $P < 0.001$; first surgical epoch: 0.137 [$0.091, 0.182$]; $P < 0.001$; second surgical epoch: 0.123 [$0.079, 0.168$]; $P < 0.001$; third surgical epoch: 0.076 [$0.031, 0.121$]; $P = 0.007$) compared to preoxygenation baseline values. Before extubation, alpha and theta connectivity returned to baseline levels.

Dynamic Patterns of Cortical Connectivity during Surgical Anesthesia

The aforementioned analysis demonstrated that cortical connectivity exhibited, on average, distinct spatial and

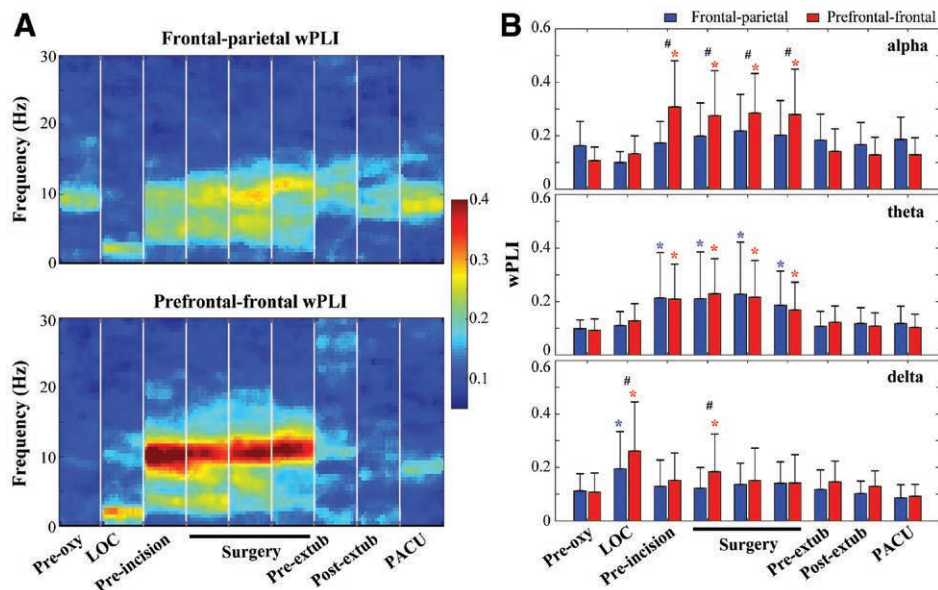


Fig. 3. Functional cortical connectivity changes across the studied epochs, as assessed by weighted phase lag index (wPLI). (A) Group-level (mean across all available patients) connectogram of the mean wPLI between frontal (F5, F6, Fz) and parietal (P5, P6, Pz) channels, and between prefrontal (Fp1, Fp2) and frontal channels. (B) The mean and SD of wPLI values at alpha (7 to 15 Hz), theta (3 to 7 Hz), and delta (0.5 to 3 Hz) bands. *Significant changes relative to the preoxygenation epoch for frontal–parietal (blue) and prefrontal–frontal (red) wPLI, respectively (Bonferroni-corrected $P < 0.05$); # significant difference between frontal–parietal and prefrontal–frontal wPLI (Supplemental Digital Content 4, fig. 1, Bonferroni-corrected $P < 0.05$), using linear mixed model analysis.

spectral properties across the studied perioperative epochs at a group level. We then investigated if the cortical connectivity, as assessed by frequency-resolved frontal–parietal and prefrontal–frontal weighted phase lag index, was static or dynamic during anesthetic maintenance in individual patients. These regions were chosen given their postulated role in consciousness and anesthetic-induced unconsciousness.^{3–6,15,16} Frontal–parietal and prefrontal–frontal connectivity were subjected to principal component analysis for dimensionality reduction and then grouped into five clusters *via* k-means clustering. In this study, the first five principal components were retained, which contained 63.1% of the total variance of the original connectivity patterns. With five principal components and five clusters, the stability index is 0.30 ± 0.08 , and the 1– minimum Hamming distance is 0.76 ± 0.07 across the different clustering solutions (see Supplemental Digital Content 2, <http://links.lww.com/ALN/B913>). This suggests that 76% of the data were allocated to the same clusters through different solutions and the clustering was 76% consistent among participants.

Each cluster (connectivity state) demonstrated its characteristic connectivity pattern with distinct spatial and spectral properties (fig. 4A, table 3). States 1 and 2 are characterized by suppressed frontal–parietal connectivity with elevated prefrontal–frontal connectivity at 10 to 20 Hz and 7 to 15 Hz, respectively, state 3 is distinguished by a predominance

of delta prefrontal–frontal connectivity, and states 4 and 5 demonstrate minimal prefrontal–frontal connectivity with high frontal–parietal connectivity at theta and alpha frequency bands separately. Based on the squared Euclidean distance with these characterized patterns, each time window was assigned to one of the five states, and those with burst suppression were grouped into an additional state as “BS,” yielding the time series of connectivity states for each participant (see Supplemental Digital Content 4, fig. 1, <http://links.lww.com/ALN/B915>). Except for a few participants with a short duration of surgery, the majority of the participants demonstrated changing frontal–parietal and prefrontal–frontal connectivity states over time. The temporal dynamics of the connectivity state time series were assessed by occurrence rate (fig. 4B) and the distribution of dwell time (fig. 4C) for each state. A certain state is not specific for a subgroup of a few participants, but rather, occurred for most of the participants. The dwell time was varied from 30s to tens of minutes among multiple visits to a certain state; for example, across all the states, the dwell time for 70.6 to 80.8% of the visits were longer than 30s, among which 8.2 to 21.3% were longer than 2 min. Overall, these results suggest that the cortical connectivity is not static, as transitions occurred among states.

State transitions were low and variable across states and participants (see Supplemental Digital Content 5, fig. 1, <http://>

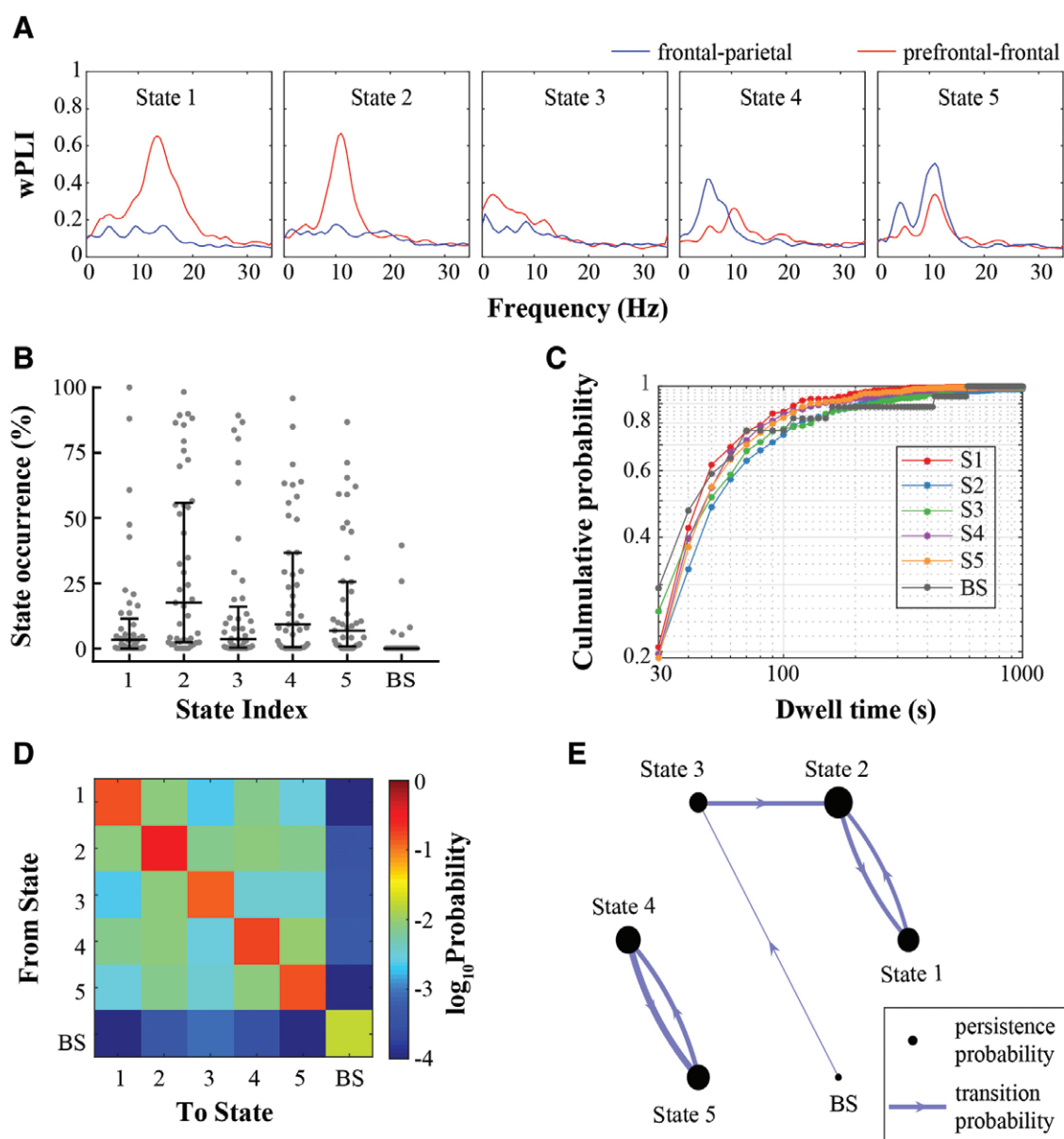


Fig. 4. Dynamic cortical connectivity during anesthetic maintenance (*i.e.*, skin incision until the last recorded minimum alveolar concentration value of 0.7 toward the end of surgery). (A) Representative connectivity states characterized by distinct spectral patterns of frontal–parietal and prefrontal–frontal weighted phase lag index from cluster analysis. (B) State occurrence rate, *i.e.*, the fraction of time spent in each connectivity state, with the central black bar and error bars indicating the median and interquartile range of the values across patients with individual values shown in gray dots. (C) Cumulative dwell time for each connectivity state across all patients. The dwell time was variable (from 30 s to a few minutes) among multiple visits to a certain state. (D) Transition probability between the connectivity states, with each element in the transition matrix indicating the probability of transitioning from any state in a given row to another state in the given column, with the element on the diagonal line indicating the probability of staying in a certain state. (E) Graphical representation of the significant state persistencies and state switches as compared to random transitions through surrogate data analysis (false discovery rate–adjusted $P < 0.05$; see Supplemental Digital Content 5, <http://links.lww.com/ALN/B916>). Each node indicates a connectivity state, the size of the node is proportional to the persistence probability in each state, and the directed, weighted edges are proportional to the transition probability between the two states. The significant probability values were estimated by the original persistence or transition probability values after subtracting the mean of those from surrogate data.

Table 3. Connectivity States

State	Dominant Frequency Range (Hz)	Predominant Region
State 1	10–20	Prefrontal–frontal
State 2	7–15	Prefrontal–frontal
State 3	0.5–3	Prefrontal–frontal
State 4	3–7	Frontal–parietal
State 5	3–15	Frontal–parietal
State BS	Burst suppression	--

BS, burst suppression.

links.lww.com/ALN/B916). Aggregated over all connectivity states, cortical connectivity demonstrated high persistency, with probability of $86.6 \pm 8.1\%$, which was significantly higher than that of switching to a different state ($13.4 \pm 8.1\%$ across all participants; $P < 0.001$). Additionally, figure 4D presents the group-level transition probability matrix using all patients, with each element indicating the probability of transitioning from any state in a given row to another state in the given column, with the element on the diagonal line indicating the probability of staying in a certain state. It is visibly evident that persistence in the same state was more probable than transitioning to a different state. When compared with the transition probability from surrogate data generated by randomly shuffling the state time series while keeping state occurrence rate, only the persistence probability on the diagonal line was significantly higher than that from surrogate data ($P < 0.05$; see Supplemental Digital Content 5, fig. 2, <http://links.lww.com/ALN/B916>). Furthermore, we focused on the between-state transitions and compared the original transition probability with that of surrogate data generated by randomly shuffling the state time series after removing the state persistencies. Analysis revealed that the transitions between states were not evenly distributed, and a few between-state transitions did happen more frequently than predicted by random occurrence ($P < 0.05$; see Supplemental Digital Content 5, fig. 3, <http://links.lww.com/ALN/B916>). Figure 4E shows the significant persistence probability and between-state transition probability. It is expected that the two states with high prefrontal–frontal connectivity (states 1 and 2) have a higher probability of transitioning into and out of each other, as do the two states with relatively higher frontal–parietal connectivity (states 4 and 5). However, across these states, only state 2 is more probable than random chance when transitioning out of the state associated with delta connectivity (state 3). In other words, it is more probable to stay in a certain connectivity state than transitioning to another state, though when transitions occur, a few between-state transitions are more probable than others.

Discussion

With this study, cortical connectivity was assessed throughout the course of surgery and general anesthesia. The results

demonstrate distinct patterns of dynamic cortical connectivity throughout the perioperative period. Alpha frontal–parietal connectivity, assessed *via* weighted phase lag index, was unable to distinguish among multiple levels of consciousness. Anesthetic-induced loss of consciousness was initially accompanied by an increase in delta connectivity between prefrontal–frontal and frontal–parietal channels, and theta connectivity—along with alpha prefrontal–frontal connectivity—were observed to gradually increase during subsequent anesthetic and surgical epochs. During the anesthetic maintenance phase specifically, connectivity shifted among neurophysiologic states with distinct oscillatory and spatial characteristics. Overall, the results suggest that brain states undergo dynamic shifts during surgery and anesthesia.

Alpha frontal–parietal connectivity, as assessed by weighted phase lag index, was unable to distinguish levels of consciousness or anesthetic states in surgical patients as a single, static measure. These findings may appear discrepant with prior studies demonstrating disrupted frontal–parietal connectivity during general anesthesia.^{6,29–33} However, frontal–parietal connectivity has often been studied as a single epoch after induction of anesthesia,^{6,26} as opposed to longer durations that parallel surgical time length (and with surgical stimulation). Indeed, if only the preoxygenation baseline and induction periods were considered, the alpha frontal–parietal connectivity decrease would have reached statistical significance (-0.063 [$-0.110, 0.016$]; uncorrected $P = 0.009$). By observing the subsequent surgical and anesthetic epochs, and correcting for multiple comparisons, dynamic connectivity changes were observed and rendered statistically insignificant compared to the baseline period. Other surrogate measures of connectivity (*e.g.*, symbolic transfer entropy^{6,31}) may have revealed different results, though weighted phase lag index was chosen given the relatively low susceptibility to volume conduction and reference montage confounding.^{11,12} Such static connectivity measures may also be unable to detect the rich network and brain state repertoire changes that occur during anesthesia.^{29,34} Additionally, frontal–parietal connectivity was measured during surgery, and noxious stimulation may modulate connectivity between anterior and posterior brain regions.^{35,36} As such, complementary analysis could

focus on frontal–parietal connectivity patterns at surgical anesthetic depths, with longer temporal duration (*i.e.*, multiple hours, to mimic surgery), and without the confound of surgical stimulation. The possibility also remains that brain states require more dynamic analysis to differentiate levels of consciousness. In fact, accumulating evidence suggests that network topology and reconfiguration, rather than single-dimensional measures of connectivity, may be required to discriminate anesthetic states.^{37–42} Indeed, connectivity values varied widely among bandwidths and neuroanatomical regions during anesthetic maintenance and surgical phases. As such, the previously described dynamic connectivity analysis was performed to further explore these connectivity dynamics with higher temporal resolution across the entire anesthetic maintenance phase.

Dynamic connectivity analysis during the anesthetic maintenance period revealed novel findings. Although brain states tended to remain within a low number of clusters, cluster transitions frequently occurred during anesthetic maintenance, even prior to surgical stimulation (see Supplemental Digital Content 4, fig. 2, <http://links.lww.com/ALN/B915>), suggesting a dynamic interplay among brain states rather than a static equilibrium. This pattern may suggest metastability during general anesthesia,⁷ though this hypothesis would require formal testing in the setting of stable anesthetic depth and without surgical stimulation. Fluctuation in prefrontal–frontal and frontal–parietal connectivity was observed during anesthetic maintenance, particularly in the alpha and theta bandwidths (fig. 4). Alpha prefrontal–frontal connectivity was more robust, given the associated persistence probability and high connectivity values during anesthesia. This may reflect thalamocortical hypersynchrony that occurs with γ -aminobutyric acid–mediated anesthetics (*e.g.*, propofol).^{16,43,44} Furthermore, these prefrontal–frontal connectivity states (1 and 2) occur during suppressed frontal–parietal connectivity, and frontal–parietal connectivity states (4 and 5) appear to emerge during relative suppression of prefrontal–frontal connectivity (fig. 4). This possible “toggling” between brain states may reflect disrupted cortical communication as frontal hypersynchrony blocks long-range communication with temporal and parietal cortices.⁴⁵ Thus, these findings may suggest a limited repertoire of connectivity states during general anesthesia, with inhibited capacity for flexibly processing or integrating information in the brain.^{29,34}

Limitations

MAC was adjusted throughout surgery as clinically indicated, rather than maintained at a constant value. Thus, neurophysiologic changes occurring during the maintenance phase may have been reflective, in part, of changing anesthetic concentrations. Nonetheless, connectivity states did not appear to correlate with anesthetic depth, variability, or maintenance regimen (see Supplemental Digital Content 3, figs. 2 and 3, <http://links.lww.com/ALN/B914>). To test more rigorously

for intrinsic brain state shifts during general anesthesia, such experiments should be conducted in the absence of surgical stimulation, shifting anesthetic depths, or multiple anesthetic agents. Surgical stimulation, in particular, also varied considerably (*e.g.*, catheter placement, skin incision, tissue excision) given procedural heterogeneity. Adjuvant medications, such as opioids, may have also impacted the underlying neurophysiology and anesthetic requirements.^{46,47} These considerations could, however, be considered a strength from the perspective of pragmatic design and generalizability. Indeed, the express goal of this investigation was to test the translational significance of past connectivity studies in the context of real-world surgery and general anesthesia. We did not have a dedicated baseline conscious period; thus, connectivity and metastability comparisons cannot be compared to a prolonged state of wakeful consciousness. Additionally, behavioral responsiveness was not assessed throughout the anesthetic maintenance phase. Our analyses were also restricted to one measure of functional connectivity (weighted phase lag index); alternative methodologies might result in different conclusions. Although frontal–parietal connectivity did not reliably appear to decrease during general anesthesia, Naci *et al.* recently demonstrated a number of complementary possibilities, including a disrupted frontal–parietal network or a maintained frontal–parietal connectivity that is functionally disconnected from sensory cortex.⁴⁸ Lastly, despite the outlined artifact-reduction and filtering strategies, artifactual contamination remains possible. Nonetheless, we have demonstrated the ability to acquire these neurophysiologic data in a pragmatic surgical setting.

Conclusions

Dynamic fluctuations in connectivity states are apparent during surgery and anesthesia, particularly involving the alpha and theta bandwidths. Thus, a single measure of connectivity is unlikely to be a reliable correlate of surgical anesthesia. Subsequent investigation is warranted to further understand the clinical and scientific relevance of the dynamic state changes observed in this study.

Research Support

Supported by the National Institutes of Health grant No. R01GM098578 (Bethesda, Maryland; to Drs. Mashour and Vlisides).

Competing Interests

The authors declare no competing interests.

Correspondence

Address correspondence to Dr. Vlisides: Department of Anesthesiology, University of Michigan Medical School, 1H247 UH, SPC-5048, 1500 East Medical Center Drive

Ann Arbor, Michigan 48109-5048. pvlsides@med.umich.edu. Information on purchasing reprints may be found at www.anesthesiology.org or on the masthead page at the beginning of this issue. ANESTHESIOLOGY's articles are made freely accessible to all readers, for personal use only, 6 months from the cover date of the issue.

References

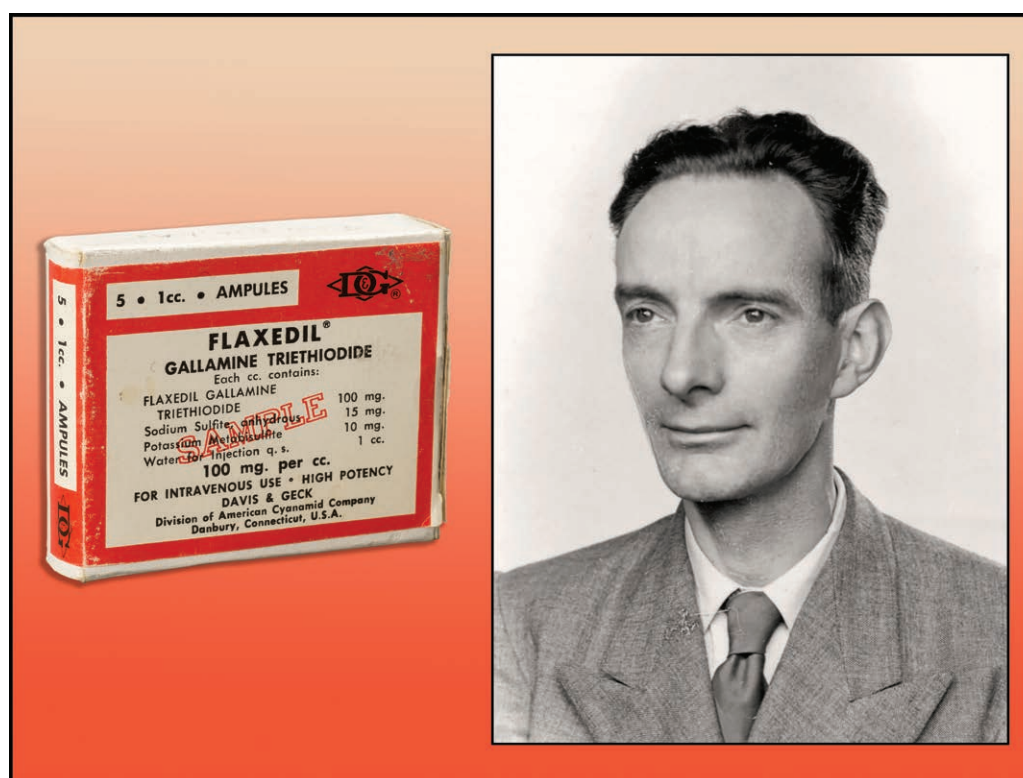
1. Akeju O, Westover MB, Pavone KJ, Sampson AL, Hartnack KE, Brown EN, Purdon PL: Effects of sevoflurane and propofol on frontal electroencephalogram power and coherence. *ANESTHESIOLOGY* 2014; 121:990–8
2. Akeju O, Pavone KJ, Westover MB, Vazquez R, Prerau MJ, Harrell PG, Hartnack KE, Rhee J, Sampson AL, Habeeb K, Gao L, Lei G, Pierce ET, Walsh JL, Brown EN, Purdon PL: A comparison of propofol- and dexmedetomidine-induced electroencephalogram dynamics using spectral and coherence analysis. *ANESTHESIOLOGY* 2014; 121:978–89
3. Boly M, Moran R, Murphy M, Boveroux P, Bruno MA, Noirhomme Q, Ledoux D, Bonhomme V, Brichant JF, Tononi G, Laureys S, Friston K: Connectivity changes underlying spectral EEG changes during propofol-induced loss of consciousness. *J Neurosci* 2012; 32:7082–90
4. Schrouff J, Perlberg V, Boly M, Marrelec G, Boveroux P, Vanhaudenhuyse A, Bruno MA, Laureys S, Phillips C, Péligrini-Issac M, Maquet P, Benali H: Brain functional integration decreases during propofol-induced loss of consciousness. *Neuroimage* 2011; 57:198–205
5. Ku SW, Lee U, Noh GJ, Jun IG, Mashour GA: Preferential inhibition of frontal-to-parietal feedback connectivity is a neurophysiologic correlate of general anesthesia in surgical patients. *PLoS One* 2011; 6:e25155
6. Jordan D, Ilg R, Riedl V, Schorer A, Grimberg S, Neufang S, Omerovic A, Berger S, Untergehrer G, Preibisch C, Schulz E, Schuster T, Schröter M, Spoormaker V, Zimmer C, Hemmer B, Wohlschläger A, Kochs EF, Schneider G: Simultaneous electroencephalographic and functional magnetic resonance imaging indicate impaired cortical top-down processing in association with anesthetic-induced unconsciousness. *ANESTHESIOLOGY* 2013; 119:1031–42
7. Hudson AE: Metastability of neuronal dynamics during general anesthesia: Time for a change in our assumptions? *Front Neural Circuits* 2017; 11:58
8. Tognoli E, Kelso JA: The metastable brain. *Neuron* 2014; 81:35–48
9. Mitra P, Bokil H: Observed brain dynamics, Oxford University Press, 2007
10. Delorme A, Makeig S: EEGLAB: An open source toolbox for analysis of single-trial EEG dynamics including independent component analysis. *J Neurosci Methods* 2004; 134:9–21
11. Vinck M, Oostenveld R, van Wingerden M, Battaglia F, Pennartz CM: An improved index of phase-synchronization for electrophysiological data in the presence of volume-conduction, noise and sample-size bias. *Neuroimage* 2011; 55:1548–65
12. Stam CJ, Nolte G, Daffertshofer A: Phase lag index: Assessment of functional connectivity from multi channel EEG and MEG with diminished bias from common sources. *Hum Brain Mapp* 2007; 28:1178–93
13. Oostenveld R, Fries P, Maris E, Schoffelen JM: FieldTrip: Open source software for advanced analysis of MEG, EEG, and invasive electrophysiological data. *Comput Intell Neurosci* 2011; 2011:156869
14. Papana A, Kugiumtzis D, Larsson PG: Reducing the bias of causality measures. *Phys Rev E Stat Nonlin Soft Matter Phys* 2011; 83(3 Pt 2):036207
15. Flores FJ, Hartnack KE, Fath AB, Kim SE, Wilson MA, Brown EN, Purdon PL: Thalamocortical synchronization during induction and emergence from propofol-induced unconsciousness. *Proc Natl Acad Sci USA* 2017; 114:E6660–8
16. Purdon PL, Pierce ET, Mukamel EA, Prerau MJ, Walsh JL, Wong KF, Salazar-Gomez AF, Harrell PG, Sampson AL, Cimenser A, Ching S, Kopell NJ, Tavares-Stoeckel C, Habeeb K, Merhar R, Brown EN: Electroencephalogram signatures of loss and recovery of consciousness from propofol. *Proc Natl Acad Sci USA* 2013; 110:E1142–51
17. Avidan MS, Jacobsohn E, Glick D, Burnside BA, Zhang L, Villafranca A, Karl L, Kamal S, Torres B, O'Connor M, Evers AS, Gradwohl S, Lin N, Palanca BJ, Mashour GA; BAG-RECALL Research Group: Prevention of intraoperative awareness in a high-risk surgical population. *N Engl J Med* 2011; 365:591–600
18. Mashour GA, Esaki RK, Vandervest JC, Shanks A, Kheterpal S: A novel electronic algorithm for detecting potentially insufficient anesthesia: Implications for the prevention of intraoperative awareness. *J Clin Monit Comput* 2009; 23:273–7
19. Hambrecht-Wiedbusch VS, Li D, Mashour GA: Paradoxical emergence: Administration of subanesthetic ketamine during isoflurane anesthesia induces burst suppression but accelerates recovery. *ANESTHESIOLOGY* 2017; 126:482–94
20. Lange T, Roth V, Braun ML, Buhmann JM: Stability-based validation of clustering solutions. *Neural Comput* 2004; 16:1299–323
21. Hudson AE, Calderon DP, Pfaff DW, Proekt A: Recovery of consciousness is mediated by a network of discrete metastable activity states. *Proc Natl Acad Sci USA* 2014; 111:9283–8
22. Vidaurre D, Abeyesuriya R, Becker R, Quinn AJ, Alfaro-Almagro F, Smith SM, Woolrich MW: Discovering

- dynamic brain networks from big data in rest and task. *Neuroimage* 2018; 180(Pt B):646–56
23. Ma S, Calhoun VD, Phlypo R, Adalı T: Dynamic changes of spatial functional network connectivity in healthy individuals and schizophrenia patients using independent vector analysis. *Neuroimage* 2014; 90:196–206
 24. Ma Y, Hamilton C, Zhang N: Dynamic connectivity patterns in conscious and unconscious brain. *Brain Connect* 2017; 7:1–12
 25. Baker AP, Brookes MJ, Rezek IA, Smith SM, Behrens T, Probert Smith PJ, Woolrich M: Fast transient networks in spontaneous human brain activity. *Elife* 2014; 3:e01867
 26. Lee U, Ku S, Noh G, Baek S, Choi B, Mashour GA: Disruption of frontal-parietal communication by ketamine, propofol, and sevoflurane. *ANESTHESIOLOGY* 2013; 118:1264–75
 27. Giattino CM, Gardner JE, Sbahi FM, Roberts KC, Cooter M, Moretti E, Browndyke JN, Mathew JP, Woldorff MG, Berger M; MADCO-PC Investigators: Intraoperative frontal alpha-band power correlates with preoperative neurocognitive function in older adults. *Front Syst Neurosci* 2017; 11:24
 28. Lancaster G, Iatsenko D, Pidde A, Ticcinelli V, Stefanovska A: Surrogate data for hypothesis testing of physical systems. *Physics Reports* 2018; 748: 1–60
 29. Uhrig L, Sitt JD, Jacob A, Tasserie J, Barttfeld P, Dupont M, Dehaene S, Jarraya B: Resting-state dynamics as a cortical signature of anesthesia in monkeys. *ANESTHESIOLOGY* 2018; 129:942–58
 30. Bonhomme V, Vanhaudenhuyse A, Demertzi A, Bruno MA, Jaquet O, Bahri MA, Plenevaux A, Boly M, Boveroux P, Soddu A, Brichant JF, Maquet P, Laureys S: Resting-state network-specific breakdown of functional connectivity during ketamine alteration of consciousness in volunteers. *ANESTHESIOLOGY* 2016; 125:873–88
 31. Ranft A, Golkowski D, Kiel T, Riedl V, Kohl P, Rohrer G, Pientka J, Berger S, Thul A, Maurer M, Preibisch C, Zimmer C, Mashour GA, Kochs EF, Jordan D, Ilg R: Neural correlates of sevoflurane-induced unconsciousness identified by simultaneous functional magnetic resonance imaging and electroencephalography. *ANESTHESIOLOGY* 2016; 125:861–72
 32. Palanca BJ, Mitra A, Larson-Prior L, Snyder AZ, Avidan MS, Raichle ME: Resting-state functional magnetic resonance imaging correlates of sevoflurane-induced unconsciousness. *ANESTHESIOLOGY* 2015; 123:346–56
 33. Boveroux P, Vanhaudenhuyse A, Bruno MA, Noirhomme Q, Lauwick S, Luxen A, Degueldre C, Plenevaux A, Schnakers C, Phillips C, Brichant JF, Bonhomme V, Maquet P, Greicius MD, Laureys S, Boly M: Breakdown of within- and between-network resting state functional magnetic resonance imaging connectivity during propofol-induced loss of consciousness. *ANESTHESIOLOGY* 2010; 113:1038–53
 34. Barttfeld P, Uhrig L, Sitt JD, Sigman M, Jarraya B, Dehaene S: Signature of consciousness in the dynamics of resting-state brain activity. *Proc Natl Acad Sci USA* 2015; 112:887–92
 35. Pavel B, Daneasa A, Rosca AE, Calin A, Zahiu D, Panaiteanu A, Zagrean AM, Zagrean L: Fronto-parietal connectivity changes following noxious stimulation during anesthesia. *J Med Life* 2014; 7:387–90
 36. Peltz E, Seifert F, DeCol R, Dörfler A, Schwab S, Maihöfner C: Functional connectivity of the human insular cortex during noxious and innocuous thermal stimulation. *Neuroimage* 2011; 54:1324–35
 37. Blain-Moraes S, Tarnal V, Vanini G, Bel-Behar T, Janke E, Picton P, Golmirzaie G, Palanca BJA, Avidan MS, Kelz MB, Mashour GA: Network efficiency and posterior alpha patterns are markers of recovery from general anesthesia: A high-density electroencephalography study in healthy volunteers. *Front Hum Neurosci* 2017; 11:328
 38. Kim H, Hudetz AG, Lee J, Mashour GA, Lee U; ReCCognition Study Group: Estimating the integrated information measure phi from high-density electroencephalography during states of consciousness in humans. *Front Hum Neurosci* 2018; 12:42
 39. Lee H, Mashour GA, Noh GJ, Kim S, Lee U: Reconfiguration of network hub structure after propofol-induced unconsciousness. *ANESTHESIOLOGY* 2013; 119:1347–59
 40. Moon JY, Lee U, Blain-Moraes S, Mashour GA: General relationship of global topology, local dynamics, and directionality in large-scale brain networks. *PLoS Comput Biol* 2015; 11:e1004225
 41. Lee U, Oh G, Kim S, Noh G, Choi B, Mashour GA: Brain networks maintain a scale-free organization across consciousness, anesthesia, and recovery: Evidence for adaptive reconfiguration. *ANESTHESIOLOGY* 2010; 113:1081–91
 42. Lee U, Mashour GA: Role of network science in the study of anesthetic state transitions. *ANESTHESIOLOGY* 2018; 129:1029–44
 43. Tinker JH, Sharbrough FW, Michenfelder JD: Anterior shift of the dominant EEG rhythm during anesthesia in the Java monkey: Correlation with anesthetic potency. *ANESTHESIOLOGY* 1977; 46:252–9
 44. John ER, Prichep LS, Kox W, Valdés-Sosa P, Bosch-Bayard J, Aubert E, Tom M, di Michele F, Gugino LD, diMichele F: Invariant reversible QEEG effects of anesthetics. *Conscious Cogn* 2001; 10: 165–83
 45. Supp GG, Siegel M, Hipp JF, Engel AK: Cortical hypersynchrony predicts breakdown of sensory processing during loss of consciousness. *Curr Biol* 2011; 21:1988–93
 46. Manyam SC, Gupta DK, Johnson KB, White JL, Pace NL, Westenskow DR, Egan TD: Opioid-volatile anesthetic synergy: A response surface model with remifentanyl

- and sevoflurane as prototypes. *ANESTHESIOLOGY* 2006; 105:267–78
47. Glass PS, Gan TJ, Howell S, Ginsberg B: Drug interactions: Volatile anesthetics and opioids. *J Clin Anesth* 1997; 9(6 Suppl):18S–22S
48. Naci L, Haugg A, MacDonald A, Anello M, Houldin E, Naqshbandi S, Gonzalez-Lara LE, Arango M, Harle C, Cusack R, Owen AM: Functional diversity of brain networks supports consciousness and verbal intelligence. *Sci Rep* 2018; 8:13259

ANESTHESIOLOGY REFLECTIONS FROM THE WOOD LIBRARY-MUSEUM

France's Daniel Bovet and Gallamine, the First Synthetic Nondepolarizing Muscle Relaxant Used Clinically



A Swiss-born Italian pharmacologist, Daniel Bovet (1907 to 1992, *right*) was a research scientist famous for discovering the first antihistamine (1937) and for synthesizing (1947) gallamine, a reversible nondepolarizing muscle relaxant. Named by the multilingual Bovet after France (Latin: *Gallia*), gallamine was synthesized in Paris by Bovet as a bulky trisquaternary curariform compound. Ironically, high doses of gallamine triethiodide (boxed and branded as Flaxedil, *left*) released histamine, which Bovet had researched previously. His success with gallamine contributed to Bovet's forsaking his 18-yr career at the celebrated Pasteur Institute for a series of research opportunities back in his family's homeland of Italy. In 1957, Bovet won the Nobel Prize in Physiology or Medicine "for his discoveries relating to synthetic compounds that inhibit the action of certain body substances, and especially their action on the vascular system and the skeletal muscles." Unfortunately, Bovet clouded his Nobel laurels in a tobacco fog about 8 yr later by publishing that individuals could raise their intelligence by smoking. (Copyright © the American Society of Anesthesiologists' Wood Library-Museum of Anesthesiology.)

George S. Bause, M.D., M.P.H., Honorary Curator and Laureate of the History of Anesthesia, Wood Library-Museum of Anesthesiology, Schaumburg, Illinois, and Clinical Associate Professor, Case Western Reserve University, Cleveland, Ohio. UJYC@aol.com.